# Tara up-regulates E-cadherin transcription by binding to the Trio RhoGEF and inhibiting Rac signaling

Tomoki Yano,[1,2] Yuji Yamazaki,[1] Makoto Adachi,[2] Katsuya Okawa,[3] Philippe Fort,[4] Masami Uji,[1] Shoichiro Tsukita,[1,2] and Sachiko Tsukita[1]

[1]Laboratory of Biological Science, Graduate School of Frontier Biosciences and Graduate School of Medicine, Osaka University, Yamadaoka 2-2, Suita, Osaka 565-0871, Japan
[2]Department of Cell Biology, Faculty of Medicine, Kyoto University, Yoshida-Konoe, Sakyo-ku, Kyoto 606-8501, Japan
[3]Drug Discovery Research Laboratories, Kyowa Hakko Kirin Co., Ltd., Nagaizumi-machi, Shizuoka, 411-8731, Japan
[4]CRBM, UMSF, Université Montpellier 2 and 1, CNRS UMR 5237, Montpellier 34293, France

The spatiotemporal regulation of *E-cadherin* expression is important during body plan development and carcinogenesis. We found that Tara (Trio-associated repeat on actin) is enriched in cadherin-based adherens junctions (AJs), and its knockdown in MDCK cells (*Tara*-KD cells) significantly decreases the expression of *E-cadherin*. *Tara*-KD activates Rac1 through the Trio RhoGEF, which binds to E-cadherin and subsequently increases the phosphorylation of p38 and Tbx3, a transcriptional *E-cadherin* repressor. Accordingly, the decrease in E-cadherin expression is abrogated by ITX3 and SB203580 (specific inhibitors of Trio RhoGEF and p38MAPK, respectively), and by dephosphomimetic Tbx3. Despite the decreased *E-cadherin* expression, the *Tara*-KD cells do not undergo an epithelial–mesenchymal transition and remain as an epithelial cell sheet, presumably due to the concomitant up-regulation of cadherin-6. *Tara*-KD reduces the actin-belt density in the circumferential ring, and the cells form flattened cysts, suggesting that Tara functions to modulate epithelial cell sheet formation and integrity by up-regulating E-cadherin transcription.

## Introduction

E-cadherin functions as a $Ca^{2+}$-dependent adhesion molecule through its extracellular region (Takeichi, 1995); its cytoplasmic portion is a cortical organizer that binds catenins and various cytoskeletal and signaling molecules (Braga, 2002; Perez-Moreno et al., 2003; Mège et al., 2006). Overall, E-cadherin is a system developer that integrates cell–cell adhesion and intracellular events to support the complex functional organization of epithelial cell sheets, which are essential in multicellular organisms (Perez-Moreno et al., 2003; Lecuit, 2005; Brembeck et al., 2006). Accumulating evidence indicates that the EMT (epithelial–mesenchymal transition)-dependent or -independent regulation of *E-cadherin* expression is critical for essential biological events, including development, differentiation, and regeneration, and for carcinogenesis (Gumbiner, 2005; Halbleib and Nelson, 2006; Jeanes et al., 2008). However, in contrast to *E-cadherin's* EMT-dependent transcriptional regulation, the EMT-independent mechanism is not well understood, although it generally occurs when epithelial sheets are modulated without their cell–cell adhesions being disrupted.

E-cadherin and other types of classical cadherins are highly enriched in the adherens junctions (AJs) and integrated into various signaling cascades, which allows epithelial cell sheets to change their configurations as required for various biological events (Wheelock et al., 2008; Nishimura and Takeichi, 2009). The mixed expression of classical cadherins changes cell–cell interactions both by homophilic interactions through the cadherins'

Dr. Shoichiro Tsukita died on 11 December 2005.

T. Yano and Y. Yamazaki contributed equally to this work.

Correspondence to Sachiko Tsukita: atsukita@biosci.med.osaka-u.ac.jp

Abbreviations used in this paper: AJ, adherens junction; CR, circumferential ring; EMT, epithelial–mesenchymal transition; GEF, guanine nucleotide exchange factor; Tara, Trio-associated repeat on actin.



The Rockefeller University Press $30.00
J. Cell Biol. Vol. 193 No. 2 319–332
www.jcb.org/cgi/doi/10.1083/jcb.201009100

extracellular domains and by altering the properties of the signal platform through their cytoplasmic domains. In this respect, the regulation of E-cadherin expression and that of other classical cadherins is critical for determining the dynamic properties of epithelial cell sheets (Perez-Moreno et al., 2003; Nishimura and Takeichi, 2009). Although the integrity of epithelial sheets is not maintained during EMT, the EMT-independent regulation of cadherin expression has recently attracted considerable attention because of its role in remodeling epithelial cell sheets without destroying the integrity of the cell sheet configuration (Wheelock et al., 2008). However, our knowledge about the EMT-independent regulation of cadherin expression is still fragmentary.

There is accumulating evidence that the ras-like GTP-binding protein (Rho) family members Rac, Rho, and Cdc42 spatiotemporally regulate the dynamic molecular organization of AJ components (Braga, 2002; Etienne-Manneville and Hall, 2002; Heasman and Ridley, 2008). A number of guanine nucleotide exchange factors (GEFs) are associated with AJs, and are thought to specify the spatiotemporally restricted actions of Rho family members (Schmidt and Hall, 2002; Otani et al., 2006). In addition, GEF-binding proteins may help specify the activities of their corresponding GEFs. However, the detailed contribution of Rho-related proteins to *E-cadherin* expression has not been reported.

Tbx3 is a member of the T-box family, a family of transcription factors with at least 22 members, each of which is involved in regulating particular developmental stages and in cancer-related processes (Papaioannou and Silver, 1998; Rodriguez et al., 2008). Although the T-box proteins are thought to be regulated downstream of WNT and/or BMP signaling pathways (Renard et al., 2007), the signaling cascades that regulate the transcriptional activity or other events downstream of the T-box proteins are not fully understood. A recent report showed that, in melanoma cells, *E-cadherin* expression is directly repressed by Tbx3 and not by EMT-related transcription factors, such as Snail and Slug (Rodriguez et al., 2008).

One prominent feature of E-cadherin is its integration into the apical belt-like AJ, with which the actin circumferential ring (CR) is associated (Yonemura et al., 1995). The AJ/CR complex is considered to play a critical role in belt-like arrangement of AJ in epithelial cells, which is spatiotemporally regulated in order to integrate various extracellular and intracellular components (Itoh et al., 1997; Perez-Moreno et al., 2003; Lecuit, 2005; Pokutta and Weis, 2007; Abe and Takeichi, 2008). Because E-cadherin– and/or other classical cadherin-based catenin/actin frameworks are distributed in cell–cell contacts, it is plausible that a critical mechanism for integrating these frameworks into the AJ/CR system exists at AJs.

Here we show that the Trio-associated repeat on actin (Tara) protein is enriched at AJs through its association with Trio RhoGEF, a binding partner of E-cadherin. In addition, Tara down-regulates the activity of Tbx3, a transcriptional suppressor of *E-cadherin*, by negatively regulating Trio's RhoGEF activity EMT independently, through a novel signaling cascade mediated by Tara/Trio/Rac1/p38/Tbx3. This finding provides a conceptually new paradigm for the regulation of E-cadherin, in which a specific signaling cascade initiated at the AJ controls the activity of a transcriptional suppressor of E-cadherin.

We also found that *Tara*-KD reduced the packing density of actin in the AJ-associated CR by decreasing the level of E-cadherin expression and concomitantly increasing the protein level of cadherin-6. We propose that Tara is a critical regulator of E-cadherin expression and that Tara modulates the properties of the cadherin-based CR and of epithelial cell sheets through its regulation.

## Results

### Tara is an AJ component that affects the levels of AJ-associated E-cadherin

In an ongoing proteomic screen of junctional fractions of the liver membrane (Tsukita and Tsukita, 1989; Yamazaki et al., 2008a), to find junctional components whose exogenous expression and/or knockdown alter the junctional levels of E-cadherin and/or claudins in cultured epithelial cells, we identified a molecule that was enriched in junctional fractions and whose knockdown decreased E-cadherin; its sequence matched that of Tara (Fig. 1 A). We then made stable knockdown cell lines of Tara by transfecting MDCK cells with a *Tara*-specific RNAi (*Tara*-KD cells). To confirm that the effects of *Tara*-KD were specific, we examined two independent constructs for *Tara*-KD, and obtained the same results. As a control for RNAi-KD, stable cell lines expressing the empty RNAi expression vector (mock transfection) were used; cell lines expressing scrambled constructions of the nucleotides for RNAi-KD were also established, and showed the same results as the mock-transfected cells (Fig. 1 D; Fig. S1 A). Immunoblotting and immunofluorescence analyses, using an anti-Tara antibody that we produced, showed that Tara colocalized with E-cadherin (Fig. 1 B; Fig. S1, B and C).

To compare the intensity of E-cadherin signals precisely between mock and *Tara*-KD cells, equal numbers of control and *Tara*-KD cells were mixed and seeded on a cover glass. In confluent sheets of *Tara*-KD cells, the E-cadherin expression was lower than in mock-transfected control cell sheets (Fig. 1, C and D), and the sheet-like configuration of the cells was maintained. In addition, the protein level of cadherin-6, the second major cadherin in MDCK cells (Stewart et al., 2000; Capaldo and Macara, 2007), was up-regulated by *Tara*-KD (Fig. 1, C and D), suggesting that the down-regulation of *Tara* at least partly induced cadherin switching in these cells. In contrast, the N-cadherin signal, which was very weak, was unchanged in the *Tara*-KD cells (unpublished data). Neither the protein levels nor the intensities of the immunofluorescent signals for cell–cell AJ-associated proteins, such as the α-, β-, and p120-catenins, occludin, and ZO-1, were altered in the *Tara*-KD cells (Fig. 1, C and E).

Consistent with these findings, thin-section electron microscopy showed that the ultrastructure of the AJ was unaffected in the *Tara*-KD cells (Fig. S1 D). Furthermore, the cell proliferation rate, in vitro wound healing, and cell–cell adhesion were all unaffected in these cells (Fig. S2, A–C). Collectively, our results indicate that knocking down *Tara* decreases the expression of E-cadherin, which is accompanied by the up-regulation of cadherin-6, without affecting the AJ-based epithelial cell sheet organization.

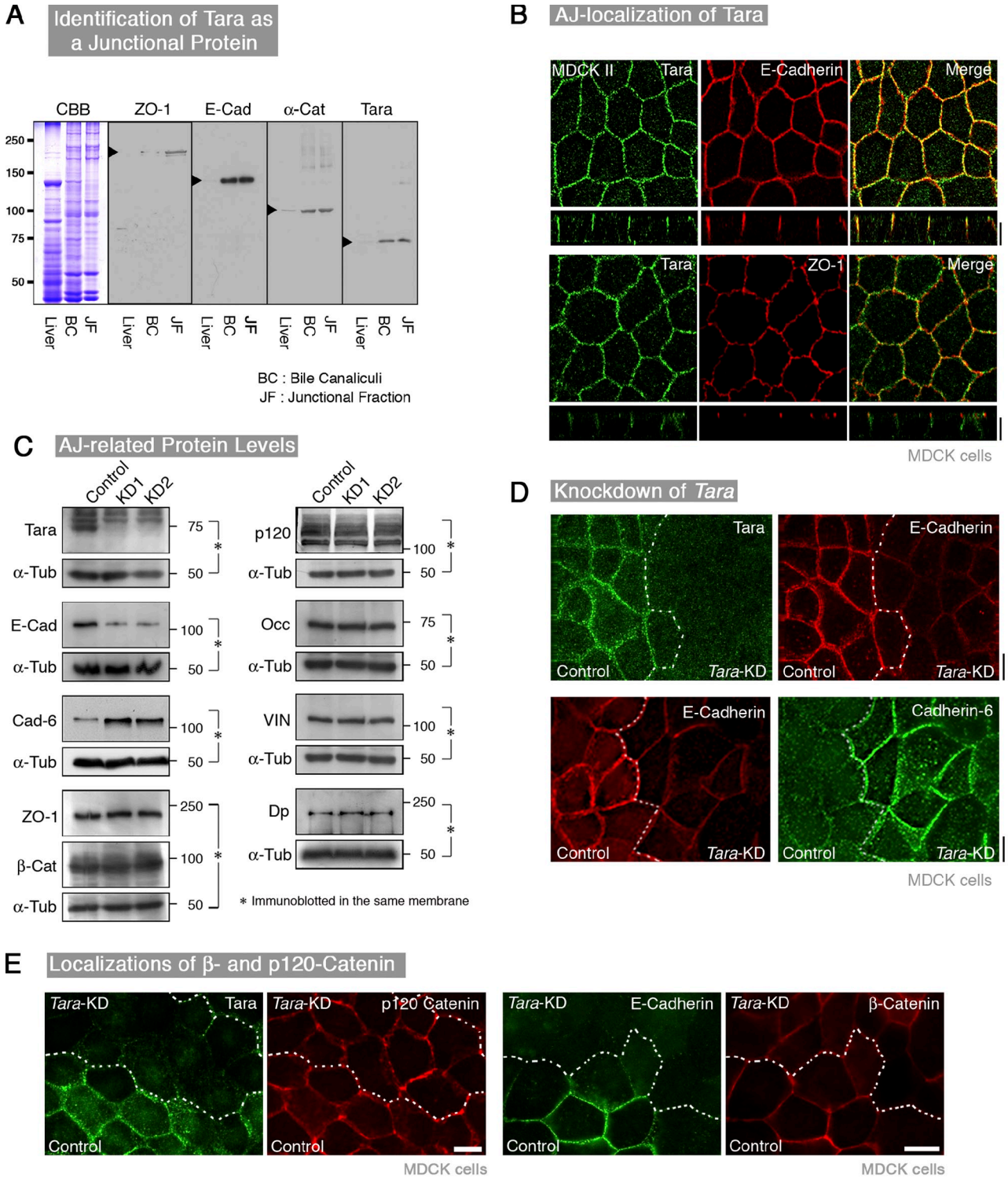


Figure 1. **Identification of Tara as an AJ component, whose knockdown down-regulates the expression of E-cadherin.** (A) Immunoblotting of the liver, bile canaliculi (BC), and the cell–cell junctional fraction (JF) with an anti-Tara antibody. Tara was enriched in the BC and JF. (B) Immunofluorescence micrographs of MDCK cells. Cells were costained for Tara with E-cadherin or ZO-1 to mark adherens or tight junctions, respectively. Top panels: Tara, green; E-cadherin, red. Bottom panels: Tara, green; ZO-1, red. Bar, 10 μm. Tara was colocalized with E-cadherin at cell–cell adherens junctions, at a position basolateral to the tight junctions. (C) Immunoblotting of *Tara*-KD and control MDCK cells (two clones) for cell–cell adhering junctional proteins. Control: mock-transfected MDCK cells. KD1 and KD2: *Tara*-KD MDCK cells (two clones). E-cad, E-cadherin; Cad-6, cadherin-6; β-Cat, β-catenin; p120, p120-catenin; Vin, vinculin; Occ, occludin; Dp, desmoplakin. Loading controls were prepared by probing portions of the same filter by anti–α-tubulin and the antibody for the respective experimental protein, except for Cad-6 and β-Cat, which were probed in the presence of the loading control anti–α-tub at the same time by mixture of antibodies. (D) Immunofluorescence micrographs of co-cultured *Tara*-KD and control mock-transfected MDCK cells stained for E-cadherin and cadherin-6. The E-cadherin signals were decreased in the *Tara*-KD cells. Note that the cadherin-6 signals were increased by *Tara*-KD. Tara, green; E-cadherin, red; cadherin-6, green (cy5-staining). Bar, 10 μm. (E) Immunofluorescence micrographs of co-cultured *Tara*-KD and control mock-transfected MDCK cells stained for p120- and β-catenins. Note that the immunofluorescence levels of the p120- and β-catenins at AJs were not changed by *Tara*-KD.

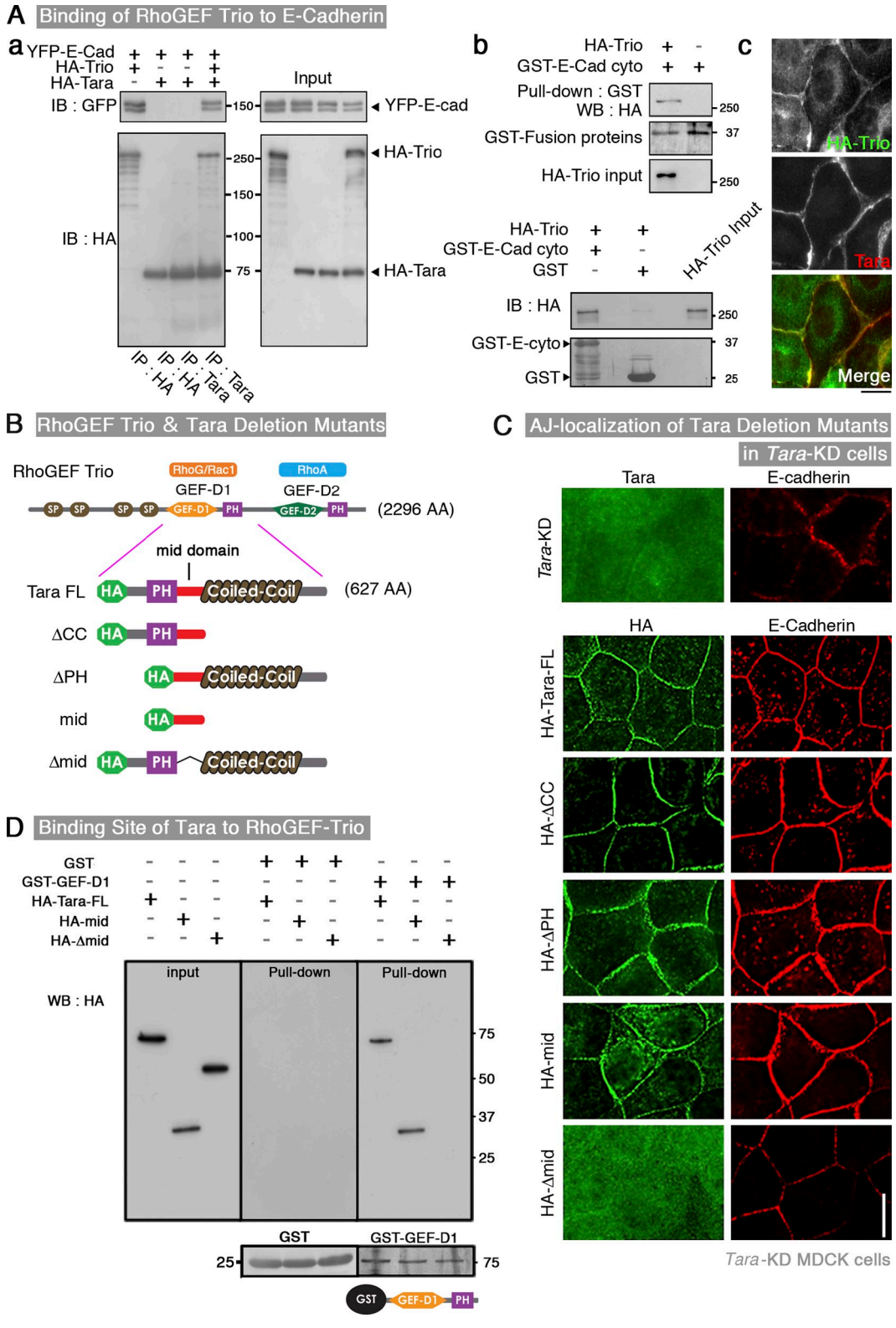


Figure 2. **Association of Tara with Trio RhoGEF, which binds E-cadherin.** (A, a) Coimmunoprecipitations among YFP-E-cadherin, HA-Trio, and HA-Tara. After the transient expression (see input) in HEK293 cells of tagged forms of Tara, E-cadherin, and Trio, a reported binding partner of Tara, YFP–E-cadherin was detected in the immunoprecipitates of HA-Tara in the presence, but not the absence, of HA-Trio. (b) Linkage between Trio and E-cadherin. HA-Trio was pulled down by a GST fusion protein of the cytoplasmic domain of E-cadherin. (c) Immunofluorescence of transiently expressed HA-Trio. The cell–cell AJs lit up, as indicated by the Tara costaining pattern. Bar, 5 µm. (B) Schematic drawing of Trio RhoGEF and the Tara deletion constructs. (C) Immunofluorescence micrographs of *Tara*-KD MDCK cells stably transfected with HA-tagged Tara deletion mutants. All the constructs except for the one lacking the mid-domain were localized to the AJ and up-regulated the immunofluorescent signals for E-cadherin. HA, green; E-cadherin, red. Bar, 10 µm. (D) Pull-down assay of full-length and mid-domain Tara, and full-length Tara lacking the mid-domain, with GST fusion proteins of the Trio RhoGEF RhoG/Rac1-GEF domain (GEF-D1) or GST (a control). The mid-domain of Tara was essential for Tara's interaction with the GEF-D1 domain.

### Molecular basis for the association of Tara with cell–cell AJs

Given the colocalization of Tara with E-cadherin, we further examined their mode of interaction. We transiently expressed tagged forms of Tara, E-cadherin, and Trio, which is a reported binding partner of Tara, in HEK293 cells and examined the binding affinities between them by coprecipitation assay. We found that Tara did not bind directly to E-cadherin, but it did bind to Trio, which bound to E-cadherin (Fig. 2 A, a). The linkage between Trio and E-cadherin was confirmed by binding experiments between Trio and a GST fusion protein of the cytoplasmic domain of E-cadherin (Fig. 2 A, b), and was consistent with the biochemical enrichment of Trio RhoGEF into the junctional fractions and AJ localization of the HA-tagged construct of Trio (Fig. 2 A, c; Fig. S2 D).

These results were in accordance with previous reports that Trio RhoGEF is associated with cadherin-11 (Kashef et al., 2009) and M-cadherin (Charrasse et al., 2007) and that Tara binds to the RhoG/Rac1-GEF domain (Trio GEF-D1) of Trio RhoGEF (Seipel et al., 2001). To address whether Trio plays a role in the junctional recruitment of Tara, we knocked down Trio in MDCK cells. We observed that the staining for Tara at AJs was lost in the *Trio* knockdown MDCK cells, suggesting that the junctional localization of Tara was dependent on the E-cadherin/Trio linkage (Fig. S2 E).

In the present study, we used mouse Tara sequence as RNAi-resistant sequence and found by immunofluorescence and pull-down analyses that the "mid-domain," between Tara's PH and coiled-coil domains, was responsible for its AJ localization and Trio RhoGEF binding (Fig. 2, B–D). In an immunofluorescence experiment using a series of Tara deletion constructs, all the constructs except the one that lacked the mid-domain increased the E-cadherin expression levels in *Tara*-KD cells, indicating that the mid-domain of Tara was required to offset the *Tara*-KD–induced down-regulation of E-cadherin (Fig. 2, B and C).

### *Tara*-KD decreases E-cadherin expression by activating Rac1

To examine *Tara*-KD's effect on epithelial cell sheets near confluence, we treated MDCK cells with EDTA/trypsin, replated them, and cultured them for 24–48 h to obtain 80–100% confluency. By immunofluorescence, E-cadherin and Tara were consistently localized to cell–cell AJs at every time point (Fig. S3 A). Moreover, when the cells were separated into insoluble and soluble fractions, both E-cadherin and Tara were predominantly recovered in the insoluble fraction, supporting the immunofluorescence results (Fig. S3 B). Immunofluorescence and immunoblotting showed that the E-cadherin levels were clearly lower in the *Tara*-KD than in the control cells at 24 and 48 h after replating (Fig. 3 A; Fig. S3 A). The *E-cadherin* mRNA was also decreased in the *Tara*-KD cells at 24 and 48 h after replating, suggesting that E-cadherin was regulated at the transcription level. In contrast, the mRNA level of *cadherin-6* did not change in the *Tara*-KD cells (Fig. 3 B). We performed a dual luciferase assay using the minimal reporter of E-cadherin and found a ∼40% decrease in reporter expression in the *Tara*-KD cells 48 h after replating (Fig. 3 C). Moreover, cycloheximide, but not MG132 (a proteolysis inhibitor), suppressed the *Tara*-KD–induced up-regulation of cadherin-6 (Fig. S3 C). These results indicate that E-cadherin is transcriptionally down-regulated by the knockdown of *Tara*, and its down-regulation is accompanied by the biosynthesis-dependent post-transcriptional increase in cadherin-6 protein. We next asked whether *Tara*-KD induced EMT. We found that the mRNA levels of EMT-related genes like *Snail*, *Slug*, *Twist*, *Zeb-1*, *Zeb-2*, *N-cadherin*, *α-smooth muscle actin*, and *vimentin* were not elevated in the *Tara*-KD cells (unpublished data), and even if *Snail* was exogenously expressed, no changes in expression of *Tara* was detected. Collectively, the decreased expression of *E-cadherin* in the *Tara*-KD cells was probably not caused by a typical EMT.

Because Tara binds the RhoG/Rac1-GEF domain (Trio GEF-D1) of Trio RhoGEF (Seipel et al., 2001), we monitored the levels of active Rac1 and RhoG in control and *Tara*-KD MDCK cells after EDTA/trypsin treatment and replating. By a conventional pull-down assay for the active form of Rac1, we found that the level of Rac1 activation was much higher in the *Tara*-KD than the control cells at 24 and 48 h after replating (Fig. 3 D), although we could not detect the activated RhoG signal in either the control or the *Tara*-KD cells (Fig. S3 D), consistent with a previous report (Backer et al., 2007). In parallel, fluorescence resonance energy transfer (FRET) analyses of Rac1 were performed to observe the spatiotemporal activation patterns in cells, using the Raichu-Rac1 probe (Fig. 3 E; Videos 1–6). Activation of Rac1 was observed at the cell–cell contacts of the control and *Tara*-KD cells, 12 and 24 h after replating. However, although active Rac1 was still easily observed at cell–cell contacts in the *Tara*-KD cells 48 h after replating, it was scarce in the control cells at this time point (Fig. 3 E; Videos 1–6). To confirm that the up-regulation of Rac1 activity in the *Tara*-KD cells was specific, we transfected these cells with full-length and deletion constructs of Tara. All of the constructs except the one lacking the mid-domain decreased the level of active Rac1 (Fig. 4, A and B) and restored the E-cadherin levels (Fig. 3 C). We also introduced a dominant-negative Rac1 into the *Tara*-KD cells, and found that it suppressed the *Tara*-KD–induced decrease in E-cadherin expression (Fig. S4 A), confirming that Tara's regulation of Rac1's activity specifically affected the *E-cadherin* expression.

### *Tara*-KD increases Rac1 activity via Trio RhoGEF, which leads to the phosphorylation of p38

To examine whether the Rac1 activity was specifically enhanced by Trio RhoGEF in *Tara*-KD cells, we used ITX3, a specific inhibitor of the Rac1-GEF activity of Trio RhoGEF (Bouquier et al., 2009). ITX3 repressed the Rac1 activity and dose dependently up-regulated the E-cadherin protein level in the *Tara*-KD cells (Fig. 4 D), thereby reversing the effects of *Tara*-KD (Fig. 4 E). The quantification of GTP-Rac1, E-cadherin, and cadherin-6 by densitometry (as shown in Fig. S4 B) in three independent experiments showed that 100 μM ITX3 significantly increased the E-cadherin expression (by 80%) in the *Tara*-KD cells compared

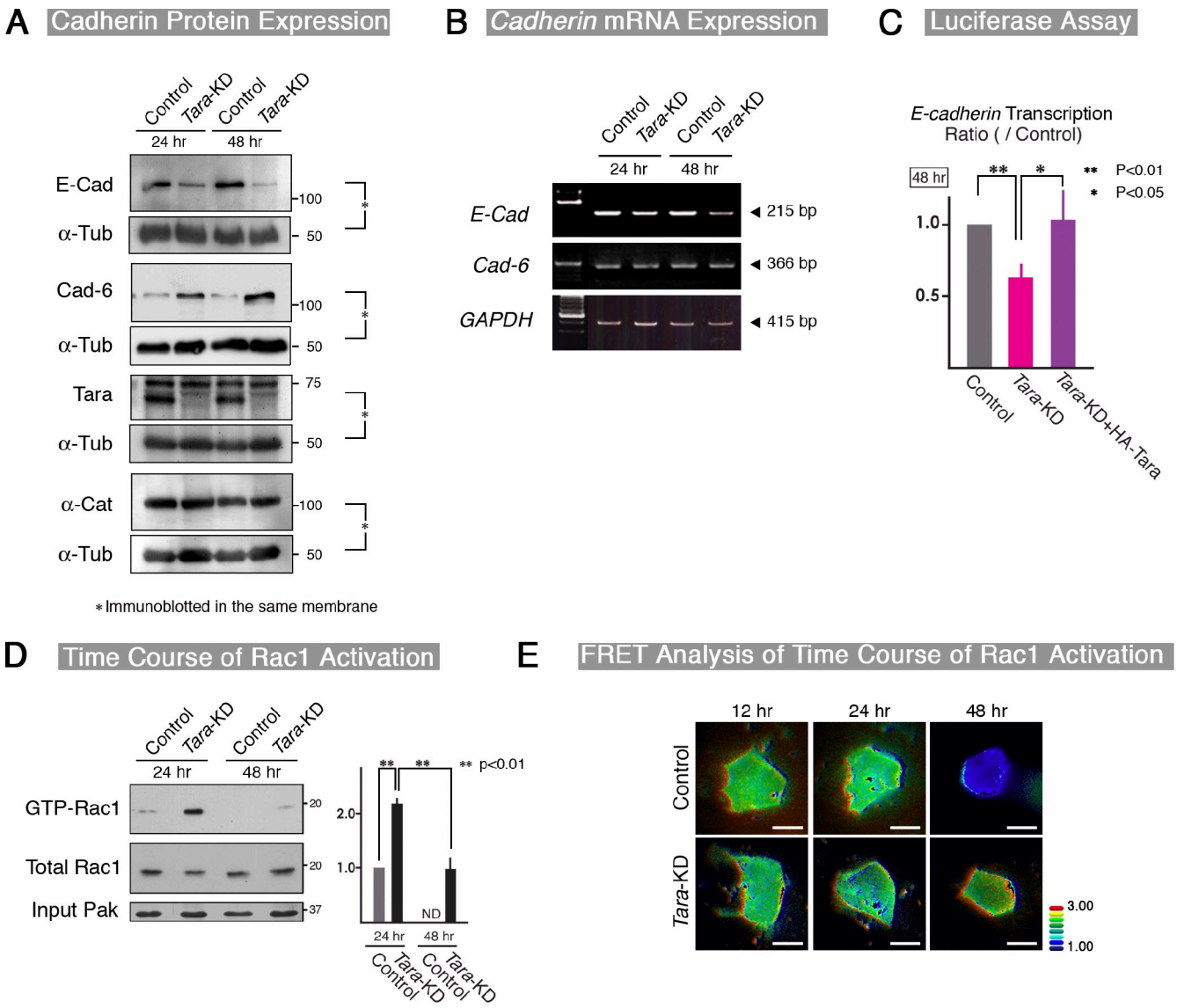


Figure 3. ***Tara*-KD–dependent regulation of E-cadherin expression and Rac1 activation.** (A) Immunoblotting of control MDCK and *Tara*-KD cells for E-cadherin, cadherin-6, and α-catenin at 24 and 48 h after EDTA/trypsin treatment and replating. Note the marked decrease in the protein level of E-cadherin by *Tara*-KD. The protein level of cadherin-6 was increased by *Tara*-KD compared with control cells. Each of E-cadherin, cadherin-6, Tara, and α-catenin was probed by its antibody in the presence of the loading control anti–α-tub at the same time by mixing antibodies. (B and C) Semi-quantitative RT-PCR (B) and luciferase reporter assays (C) for the effect of *Tara*-KD on *E-cadherin* mRNA levels and promoter activity, respectively. Note that the *E-cadherin* mRNA and its promoter activity, respectively, decreased significantly at 48 h after cells were seeded (B and C), whereas there was no obvious change in the *cadherin-6* mRNA level (not depicted). The results are expressed as means ± SD (error bars) and are representative of four independent experiments. **, $P < 0.01$; *, $P < 0.05$. (D) Effect of *Tara*-KD on the level of active Rac-1 determined by a PAK pull-down assay. The Rac1 activity was increased in *Tara*-KD cells 24 h after replating. The quantification of the immunoblotted signals revealed the significant changes of Rac1 activation by *Tara*-KD at 24 and 48 h after being seeded (see the right panel). ND, not detected. Densitometric quantification of Western blot bands was performed using Photoshop 7.0 (Adobe). As to the "Relative Intensity," the ratio of intensity of GTP-Rac1 to total-Rac in control was normalized to 1.0. The results are expressed as means ± SD (error bars) and are representative of three independent experiments. **, $P < 0.01$; *, $P < 0.05$. (E) FRET analysis of Rac activation. At 12 and 24 h after replating, the Rac1 activation was detected at cell–cell contacts in both control and *Tara*-KD cells. At 48 h, Rac activation was still detectable in *Tara*-KD cells but not in control cells. Bar, 10 µm.

with untreated *Tara*-KD cells (Fig. 4 E). To complement the Trio inhibitor data with an independent maneuver that targets Trio, we knocked down *Rac1* or *Trio* in the *Tara*-KD cells and found that the E-cadherin expression was recovered (Fig. S4, C and D). These results indicate that the Trio RhoGEF-mediated Rac1 activation specifically decreased the E-cadherin expression. Together, our findings support the idea that AJ-associated Tara/Trio RhoGEF spatiotemporally regulates Rac1 activity to alter the expression level of *E-cadherin*.

Because the Trio RhoGEF-dependent Rac1 activation was specifically up-regulated in *Tara*-KD cells, we sought to identify the signaling cascade that linked the Rac1 activation to the decreased E-cadherin expression. In this respect, Rac1 activation regulates MAP kinases such as ERK, JNK, and p38 (Rygiel et al., 2008; Zhang et al., 2009). We therefore examined the phosphorylation levels of these MAP kinases by immunoblotting, using antibodies specific for their phosphorylated form. We found that the phosphorylation level of p38 was up-regulated in the *Tara*-KD

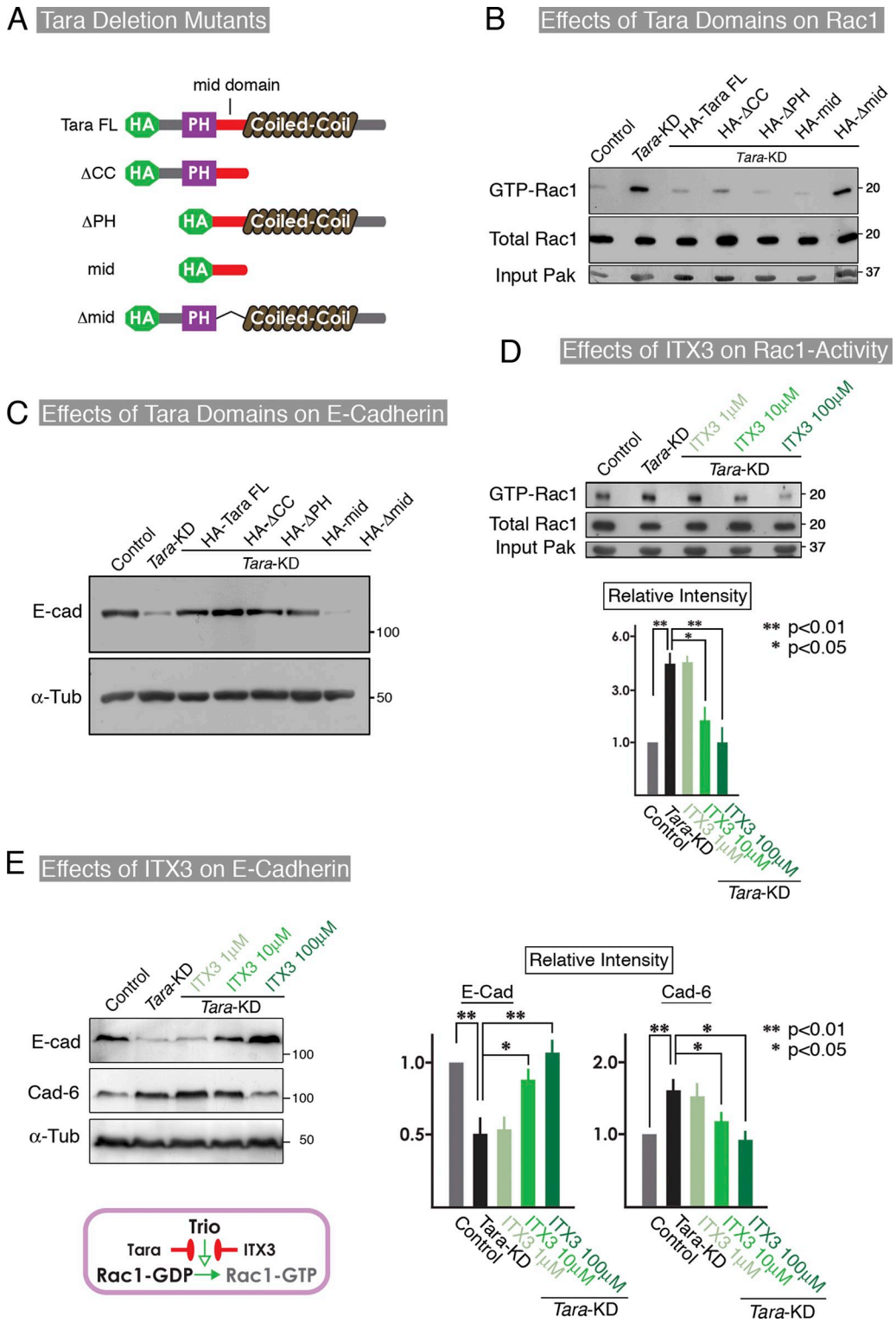


Figure 4. **Involvement of Trio in *Tara*-KD–dependent regulation of E-cadherin expression and Rac1 activation.** (A) Schematic drawing of the Tara deletion constructs. (B) The Tara domain responsible for regulating the activation of Rac1. The mid-domain of Tara was sufficient to cause the down-regulation of Rac1 activation in *Tara*-KD cells. (C) Analysis of the Tara domain responsible for the restoration of E-cadherin in *Tara*-KD cells, by transfection with Tara deletion mutants. Consistent with the Rac1 activity, the mid-domain of Tara was essential to rescue the expression of E-cadherin in *Tara*-KD cells. (D) Effect of the Trio RhoGEF inhibitor ITX3 on the activation level of Rac1 in *Tara*-KD cells. In the presence of 100 μM ITX3, the Rac1 activation in *Tara*-KD cells was markedly decreased, to the level in control cells. The results are expressed as means ± SD (error bars) and are representative of three independent experiments. **, $P < 0.01$; *, $P < 0.05$. Densitometric quantification of Western blot bands was performed using Photoshop 7.0 (Adobe). As to the "Relative Intensity," the ratio of intensities of E-cadherin to α-tubulin and cadherin-6 to α-tubulin in control were normalized to 1.0. (E) Effect of ITX3 on the expression of E-cadherin and cadherin-6 in *Tara*-KD cells. ITX3 blocked the *Tara*-KD–induced down-regulation of E-cadherin and up-regulation of cadherin-6 in a dose-dependent manner. The right panels show the quantification of the immunoblotting data (as shown in Fig. S4 C). The results are expressed as means ± SD (error bars) and are representative of three independent experiments, in which antigens were immunoblotted in the same membranes. **, $P < 0.01$; *, $P < 0.05$.

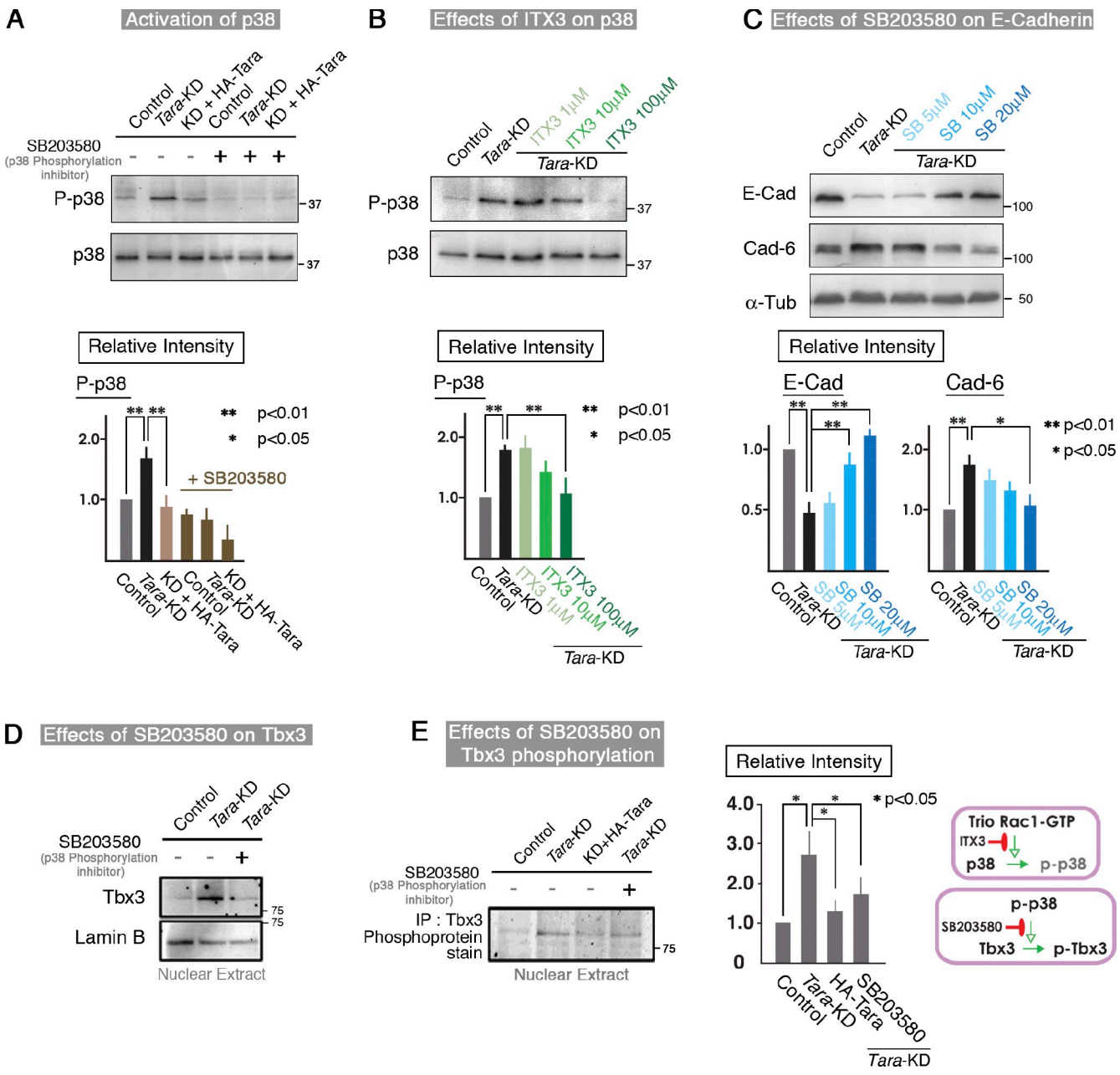


Figure 5. ***Tara-KD* regulates the p38MAPK/Tbx3 pathway downstream of Rac1.** (A and B) Immunoblotting for phospho-p38MAPK in *Tara*-KD cells in the presence or absence of SB203580 (A) or ITX3 (B). The phosphorylation level of p38MAPK was markedly up-regulated in *Tara*-KD cells compared with control cells. SB203580, a p38MAPK phosphorylation inhibitor, dose dependently decreased the phosphorylation level of p38, as did ITX3, an inhibitor of the Rac1-GEF activity of Trio RhoGEF. The bottom panels show the quantification of the immunoblotting data (as shown in Fig. S4 C). The results are expressed as means ± SD (error bars) and are representative of three independent experiments. **, $P < 0.01$; *, $P < 0.05$. Densitometric quantification of Western blot bands was performed using Photoshop 7.0 (Adobe). As to the "Relative Intensity," the ratio of intensities of P-p38 to p38 in control was normalized to 1.0. (C) Immunoblotting for E-cadherin and cadherin-6 in *Tara*-KD cells. The *Tara*-KD–induced decrease of E-cadherin and increase of cahderin-6 were dose dependently inhibited by the presence of SB203580. The bottom panels show the quantification of the immunoblotting data (Fig. S4 C). The basically same results were obtained with another inhibitor of p38, SB202190. The results are expressed as means ± SD (error bars) and are representative of three independent experiments, in which antigens were immunoblotted in the same membranes. **, $P < 0.01$; *, $P < 0.05$. Densitometric quantification of Western blot bands was performed using Photoshop 7.0 (Adobe). As to the "Relative Intensity," the ratio of intensities of E-cadherin to α-tubulin and cadherin-6 to α-tubulin in control were normalized to 1.0. (D) Immunoblotting of nuclear extracts of *Tara*-KD and control cells for Tbx3. The amount of nuclear Tbx3 in the *Tara*-KD cells was higher than that in the control cells. SB203850 blocked the increase in nuclear Tbx3 in the *Tara*-KD cells to the control level. (E) The phosphorylation level of nuclear Tbx3 was approximately fourfold increased in the *Tara*-KD cells compared with control cells, and the transfection of HA-Tara or the addition of SB203580 suppressed the increased Tbx3 phosphorylation level by ∼50%. The results are expressed as means ± SD (error bars) and are representative of three independent experiments. **, $P < 0.01$; *, $P < 0.05$.

cells compared with controls (Fig. 5 A). When the Trio RhoGEF-mediated Rac1 activity was repressed by ITX3 in the *Tara*-KD cells, the phospho-p38 signal decreased (Fig. 5 B). Therefore, the Trio RhoGEF-mediated activation of Rac1 apparently increased the phosphorylation of p38. Consistent with this scenario, SB203580, an inhibitor of p38 phosphorylation, suppressed the

*Tara*-KD–induced down-regulation of E-cadherin in a dose-dependent manner (Fig. 5 C). Quantification by densitometry (Fig. 5 C; Fig. S4 B) showed that the E-cadherin signal was significantly higher in the SB203580-treated cells (~100% increase with 10 and 20 µM SB203580). Furthermore, when SB202190 was used to inhibit the activity of p38 (Fig. 5 C; Fig. S4 E), almost the same results were obtained as those by SB203580. Thus, it is likely that Trio RhoGEF-mediated Rac1 activation increases the phosphorylation of p38, leading to a decreased level of E-cadherin in *Tara*-KD cells.

### *Tara*-KD–based phosphorylation of p38 phosphorylates Tbx3, a transcriptional repressor of *E-cadherin* that functions downstream of Tara/Trio/Rac1/p38

We next investigated how the phosphorylation of p38 decreases the expression of *E-cadherin*. After the EMT-related transcription factors had been excluded, the T-box protein family seemed the most likely candidates (Rodriguez et al., 2008). Among them, Tbx2 is reported to be phosphorylated by p38 (Abrahams et al., 2008), which suggested that Tbx2 could be a downstream effector of Tara/Trio/Rac1/p38. However, we did not detect Tbx2 signals in MDCK cells by immunoblotting, although we did detect Tbx3, which is the most closely related T-box member to Tbx2 (Papaioannou and Silver, 1998). Furthermore, the protein level of Tbx3 was increased in the nuclei as well as in whole *Tara*-KD cells compared with control cells, and this effect was counteracted by SB203580, the p38 phosphorylation inhibitor (Fig. 5 D). When we immunoprecipitated Tbx3 from nuclear extracts and analyzed it using a phosphoprotein detection kit, we found that its phosphorylation was elevated in the *Tara*-KD cells, but SB203580 reduced this effect (Fig. 5 E). These results indicated that Tbx3 is a downstream target of Tara/Trio/Rac1/p38 and that the phosphorylation and dephosphorylation of Tbx3 are critical for the transcriptional control of E-cadherin.

### The phosphorylation of Tbx3 decreases the transcription of *E-cadherin* downstream of Tara/Trio/p38, and cadherin-6 is up-regulated

To examine the involvement of Tbx3 phosphorylation in the transcriptional control of *E-cadherin*, we analyzed the effects of a dephosphomimetic Tbx3 on the *Tara*-KD–induced decrease in *E-cadherin*. The likely phosphorylation sites on Tbx3 were deduced by comparing its amino acid sequence with that of Tbx2 (Fig. 6 A), for which three phosphorylation sites have been reported: S336, S623, and S675 (Abrahams et al., 2008). There were two corresponding serine residues in Tbx3 (S334 and S692 with no candidate for S623) that might be phosphorylated. Of these, Tbx3 (S692A) had a dominant-negative effect on Tbx3's transcriptional repression of *E-cadherin* expression in *Tara*-KD cells, and the dephosphomimetic mutation of this serine in Tbx3 increased the signals for E-cadherin in the *Tara*-KD cells as shown in immunofluorescence and immunoblotting, respectively (Fig. 6, A and B). These findings led us to conclude that Tbx3 is activated by phosphorylation downstream of p38 to transcriptionally repress *E-cadherin*.

In the *Tara*-KD cells, although E-cadherin was decreased, the levels of the β- and p120-catenins were unchanged. Because the β- and p120-catenins, respectively, control the ER exit and plasma membrane association of classical cadherins (Chen et al., 1999; Ireton et al., 2002), these findings led us to hypothesize that the translation of cadherin-6, another classical cadherin that is expressed in MDCK cells, was controlled downstream of the *E-cadherin* transcription. We therefore knocked down *E-cadherin* in MDCK cells, and found that the level of cadherin-6 increased (Fig. 6 C). Furthermore, the protein levels of the β- and p120-catenins did not change in the *E-cadherin*-KD MDCK cells, suggesting there were no changes in the association of the classical cadherins with the ER exit or plasma membrane. Hence, if the protein expression of one classical cadherin decreases, the other cadherins have more p120 available to them, and their levels rise, which is referred to as "p120 sharing." In the present case, the cadherin switching was probably driven by the transcriptional control of *E-cadherin* expression. That is, when E-cadherin transcription decreased, the unchanged levels of p120- and β-catenins drove the concomitant up-regulation of cadherin-6, which does not conform to the more canonical EMT-like mechanisms.

### *Tara*-KD affects the organization of the CR

We next investigated the role of the decrease in E-cadherin and increase in cadherin-6 at the AJs in MDCK cells. Because AJs are highly organized into belt-like arrangement by the peripheral actin structure in epithelial cells, which forms the CR, we carefully examined the actin intensities at E-cadherin–rich AJs in control and *Tara*-KD MDCK cell sheets by confocal fluorescence microscopy (Fig. 7, A–C). To compare the actin intensities precisely between them, equal numbers of control and *Tara*-KD cells were mixed and seeded on a cover glass. Actin staining with rhodamine-phalloidin was less intense in the *Tara*-KD MDCK cells than in control cells. The actin intensity was restored to normal when exogenous Tara or E-cadherin was expressed in the *Tara*-KD MDCK cell sheets (Fig. 7, B and C). Furthermore, because the actin CRs form in association with the AJs, we examined the CRs stereoscopically by scanning electron microscopy (Fig. 7 D). At the AJs of control MDCK cell sheets, the actin filaments were closely packed into CRs. In contrast, the packing density of the actin filaments in the CRs was decreased in the *Tara*-KD MDCK cells. These findings suggested that the E-cadherin–based junctional actin filaments of CRs, which cooperate to organize the total AJ, are more densely packed at AJs than are the cadherin-6–based ones.

To further explore the biological relevance of Tara we used various morphogenetic approaches because E-cadherin is generally involved in morphogenesis. Among our trials, we observed *Tara*-KD–dependent morphogenetic phenotypes in three-dimensional (3D) cultures of control and *Tara*-KD MDCK cells (Fig. 7 E; Fig. S5). Control MDCK cells formed spherical cysts in collagen gels with Y/X ratios (length/width radii) of nearly 1.0 and Z/X ratios (vertical/horizontal radii) of 0.92 ± 0.07. In contrast, the *Tara*-KD MDCK cells formed 3D cysts that were more elliptical, with Z/X ratios of 0.62 ± 0.08. Immunofluorescence microscopy revealed that, although the intensity of the apical actin remained unchanged in the *Tara*-KD cells, the intensity of actin

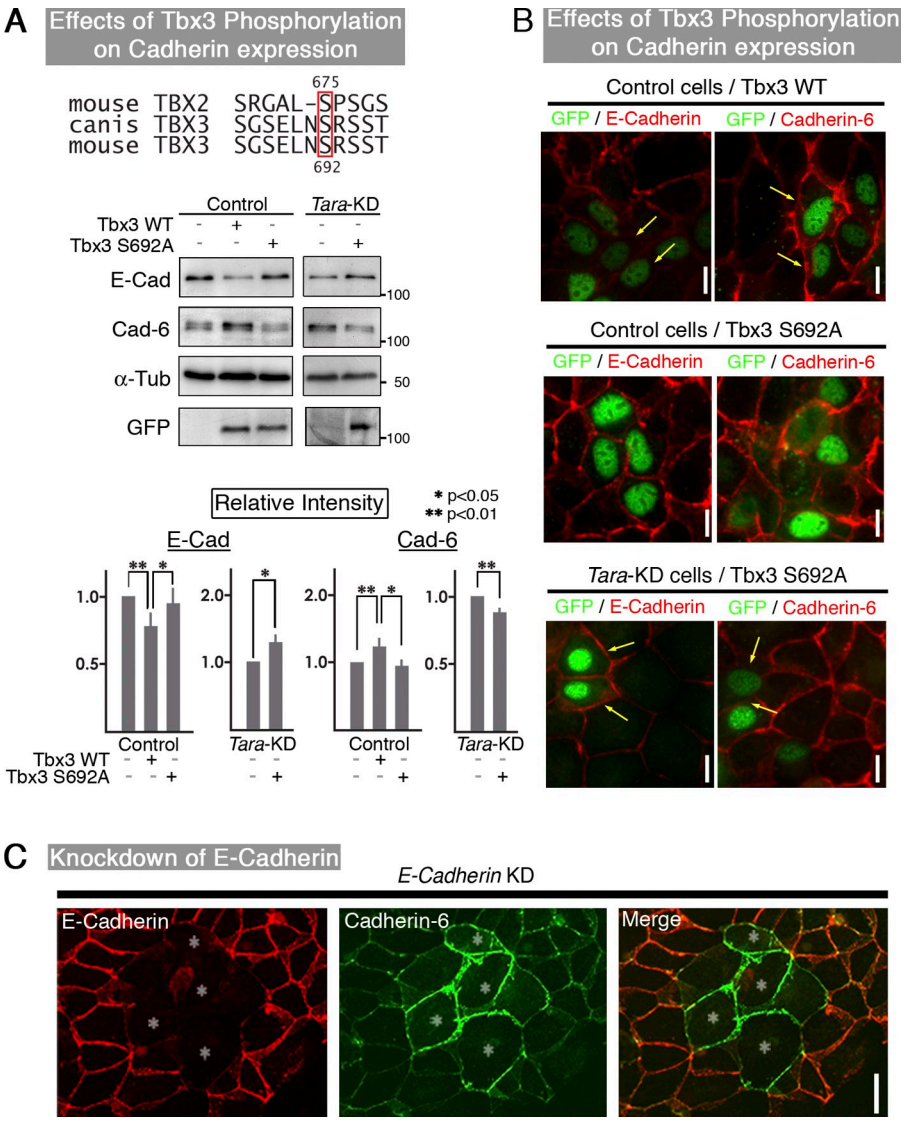


Figure 6. **Tbx3-dependent *E-cadherin* expression whose decrease leads to increased cadherin-6.** (A and B) Tbx3-dependent E-cadherin expression in MDCK cells and *Tara*-KD cells. Mouse S692 of Tbx3 (outlined in red) was the predicted phosphorylation site, based on its conservation with S675 of mouse Tbx2. As shown in immunoblotting of stable clones (A) and immunofluorescence micrographs of transient transfectants (with green nuclei, B), when exogenous wild-type Tbx3 was expressed in MDCK cells, the E-cadherin expression was decreased, and the cadherin-6 expression increased concomitantly. The dephosphomimic Tbx3 (Tbx3-S692A) showed no inhibition of E-cadherin expression (A). When exogenous wild-type Tbx3 was expressed in MDCK cells, the E-cadherin expression was decreased, and the cadherin-6 expression increased concomitantly. The dephosphomimic Tbx3 (Tbx3-S692A) showed no inhibition of E-cadherin expression. The dephosphomimetic Tbx3 suppressed the down-regulation of E-cadherin and the up-regulation of cadherin-6 in *Tara*-KD cells. Densitometric quantification of Western blot bands was performed using Photoshop 7.0 (Adobe). As to the "Relative Intensity," the ratio of intensities of E-cadherin to α-tubulin and cadherin-6 to α-tubulin in control were normalized to 1.0. The results are expressed as means ± SD (error bars) and are representative of three independent experiments, in which antigens were immunoblotted in the same membranes. **, P < 0.01; *, P < 0.05. The transfected cells are the ones with green nuclei. Bar, 10 µm. (C) Knockdown of *E-cadherin* in MDCK cells. E-cadherin, red; cadherin-6, green (cy5-staining). Bar, 10 µm. When the immunofluorescent signals of E-cadherin were decreased by *E-cadherin*-KD in MDCK cells, those for cadherin-6 increased.

and E-cadherin at the AJs and lateral membranes of the *Tara*-KD MDCK cell cysts decreased relative to the intensities in control cysts. Collectively, these findings indicate that Tara probably plays a role in fine-tuning the actin-based tension through the AJs.

## Discussion

E-cadherin is acknowledged to play critical roles in numerous biological events (Perez-Moreno et al., 2003; Lecuit, 2005; Brembeck et al., 2006), which has spurred considerable interest in researching E-cadherin–related signaling pathways with a particular emphasis on their diversity and specificity. Here, we identified a novel, specific signaling pathway, Tara/Trio/Rac1/p38/Tbx3/E-cadherin. In this pathway, Tara functions as an AJ component and a binding partner of RhoG/Rac1GEF-Trio, which up-regulates the transcription of *E-cadherin* (Fig. 7 F). In this signaling system, the *Tara*-KD–induced down-regulation of *E-cadherin* transcription is independent of EMT in the MDCK cells, which express Tbx3. Because the Tbx3-dependent regulation of *E-cadherin* transcription apparently occurs in many important biological events, future studies should examine whether the Tara/Trio/Rac1/p38/Tbx3 signaling cascade is involved in these cases. An important aspect of the current findings is that the initiation of an *E-cadherin* regulatory signal at the AJ is conceptually new.

The current work reveals a mechanism by which Rac can reduce E-cadherin activity. The source of the Rac activation signal is often not clear (Lozano et al., 2008; Hage et al., 2009), and Rac1 signaling as it pertains to cadherins is still largely unknown. In this context, many GEFs are known to be directly or indirectly associated with cadherins. In particular, Trio RhoGEF is reported to bind M-cadherin and cadherin-11 (Charrasse et al., 2007; Kashef et al., 2009), which play distinct roles in development through Rac1-related signaling. However, the details of the signaling pathways that use RhoG/Rac1 GEF-Trio are still fragmentary.

In the present study, we showed for the first time that the Trio RhoGEF-dependent Rac1 signaling that down-regulates E-cadherin transcription was dampened by Tara through an interaction between the mid-domain of Tara and the RhoG/Rac1-GEF domain of Trio. In this respect, Trio bound to the cytoplasmic domain of E-cadherin, and Trio knockdown decreased the level of Tara at AJs. It is possible that Rac1 activation is at least partly mediated by *Tara*-free E-cadherin–associated Trio RhoGEF.

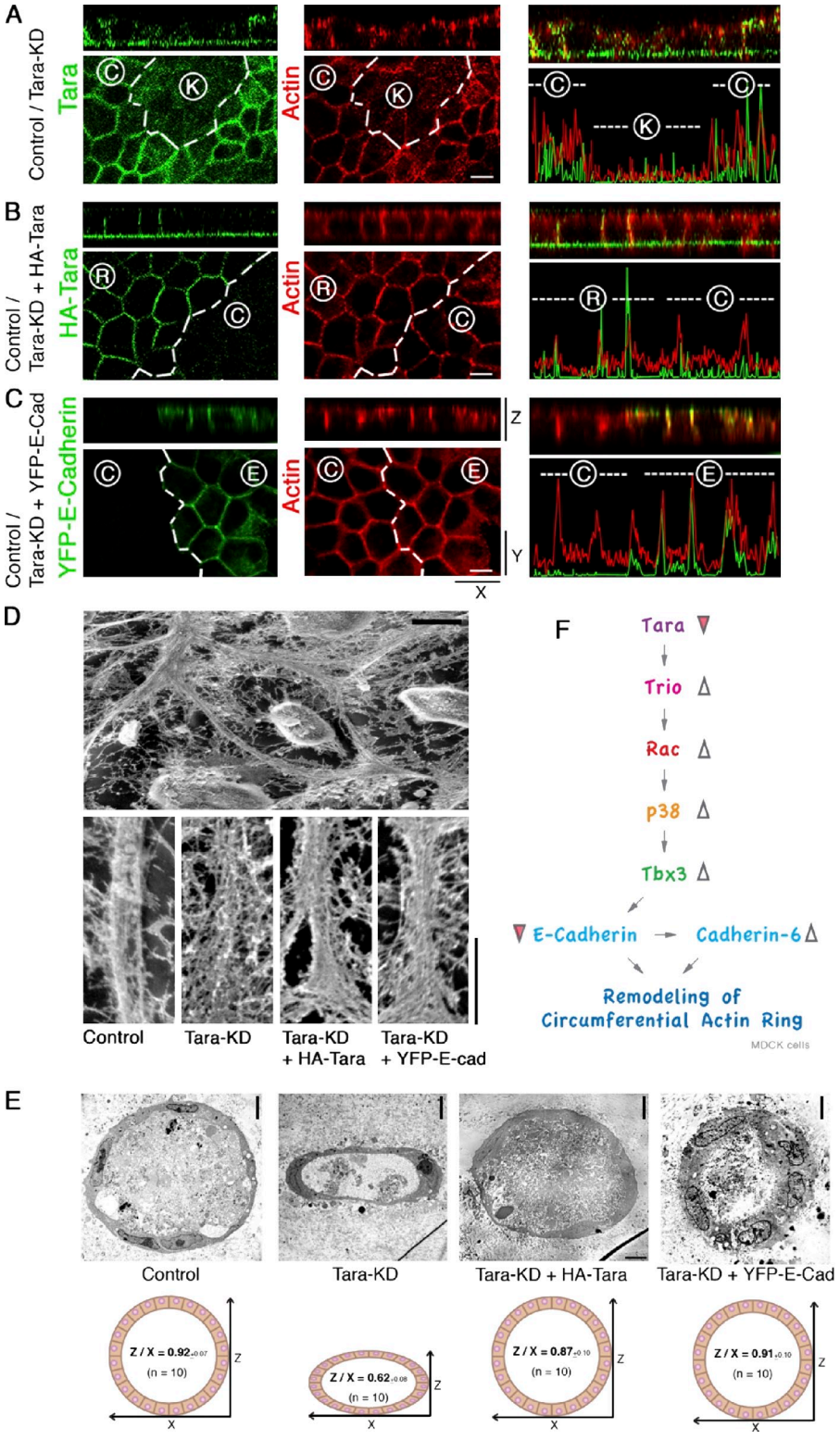


Figure 7. ***Tara*-dependent maturation of the circumferential ring.** (A–C) Confocal immunofluorescence micrographs of *Tara*-KD cells with or without transfection of HA-Tara or YFP–E-cadherin cultured with untransfected control MDCK cells. In co-cultures of control and *Tara*-KD cells, the *Tara*-KD cells showed a lower actin signal intensity at the zAJ/CR and cell–cell contacts than the control cells (A). In contrast, *Tara*-KD cells transfected with HA-Tara (B) or YFP-E-cadherin (C) exhibited actin signal intensities similar to the control cells. Bar, 10 µm. (A and B) HA, green; actin, red. (C) YFP, green; actin, red. (D) Scanning electron micrographs of *Tara*-KD cells with or without transfected HA-Tara or YFP–E-cadherin. The actin filaments of the CR were more loosely packed in the *Tara*-KD cells compared with the control cells. HA-Tara or YFP–E-cadherin partially restored the packing density of the CR actin filaments. Bar, 5 µm. (E) Electron micrographs of 3D cultures (cysts) of control cells and *Tara*-KD cells with or without transfection of HA-Tara or YFP–E-cadherin. Thin-section electron micrographs revealed that the spherical cell cysts were composed of a single-layered sheet of epithelial cells. Bar, 2 µm. The vertical-to-horizontal (Z/X) ratio of the diameters of control cell cysts was 0.92 ($n$ = 10). The *Tara*-KD cell cysts were elliptical, and *Tara*-KD cells expressing exogenous HA-Tara or YFP–E-cadherin formed spherical cell cysts similar to the control cells. The Z/X ratios of the cell cysts made by *Tara*-KD cells, *Tara*-KD cells expressing HA-Tara, or *Tara*-KD cells expressing YFP–E-cadherin were 0.62, 0.87, and 0.91, respectively ($n$ = 10). (F) Schematic drawing of the novel Tara/Trio RhoGEF/Rac1/p38MAPK/Tbx3/E-cadherin signaling cascade proposed here. This Tara/Trio/Rac1/p38/Tbx3 signaling cascade is the first E-cadherin–based AJ-initiated signal reported to regulate the transcription of *E-cadherin* in epithelial cell sheets. Here we found that Tara is enriched at AJs through its association with Trio RhoGEF, a binding partner of E-cadherin. By negatively regulating the RhoGEF activity of Trio in an EMT-independent manner, Tara down-regulates the activity of Tbx3, a transcriptional suppressor of *E-cadherin*. Furthermore, we found that *Tara*-KD remodeled the actin CR by decreasing the level of E-cadherin expression, although the protein level of cadherin-6 increased. We propose that Tara is a critical regulator of E-cadherin expression, and through this regulation Tara fine-tunes the cadherin-based actin CR and other properties of epithelial cell sheets.

Tara functions to maintain E-cadherin transcription by spatiotemporally inhibiting Rac activation in cell–cell adhesion-based events through the Tara/Trio RhoGEF/Rac1/p38/Tbx3 signaling cascade. The relationship of Rac1 to E-cadherin activity has been poorly understood, and this work adds new insight to the story.

Interestingly, Trio RhoGEF is reportedly anchored to LAR (Debant et al., 1996), a transmembrane protein with a phosphatase domain in its cytoplasmic region that binds β- and γ-catenin. This finding suggests that LAR-related signals may modulate the link between Tara and Trio RhoGEF, to activate its Rac1-GEF activity. It is also possible that cell–cell adhesion-based signals modulate the link between Trio RhoGEF and E-cadherin, which will be a subject of future study.

Although the general idea that Rac1 activation alters the localization and/or the total protein level of E-cadherin in cells is being established (Lozano et al., 2008; Hage et al., 2009), this is the first example of Rac1 regulating the transcription of *E-cadherin*, as indicated by our finding that Trio RhoGEF-based Rac1 activity up-regulates the phosphorylation level of p38 independent of EMT, to down-regulate *E-cadherin* transcription. This function of the Rac1/p38 pathway may have conceptual implications for understanding Rac1/p38 pathways in general because only a few cases involve a signaling route from p38 to cadherins, and in these cases, the phosphorylation of p38 was reported to affect the post-transcriptional down-regulation of cadherins (Zohn et al., 2006; Khanna et al., 2010). Recently, p38 was reported to phosphorylate Tbx2 (Abrahams et al., 2008), and Tbx2/3 were reported to down-regulate the transcription of *E-cadherin* (Rodriguez et al., 2008). However, these distinct events have not been linked, as they have been in this study, where we show that Rac1/p38 directly regulates the transcription of *E-cadherin*.

Despite the decreased expression of E-cadherin caused by the *Tara* knockdown, the *Tara*-KD cells did not induce an EMT, and retained their configuration as an epithelial cell sheet, presumably because of the concomitant up-regulation of cadherin-6. These findings were reminiscent of "cadherin switching," the phenomenon in which two or more cadherins show a seesaw pattern of protein expression, although cadherin switching under non-EMT circumstances is relatively undocumented (Wheelock et al., 2008). In this respect, transfection of Snail did not show any influence on the expression of *Tara* (Ikenouchi et al., 2003; unpublished data). Our present data show a detailed example of molecular signaling mechanisms leading to cadherin switching in a non-EMT situation.

A final issue relates to the cadherin-based junctional CR. Classical cadherins, with which β-catenin is associated, are linked to the CR through α-catenin/eplin/actin (Abe and Takeichi, 2008). Our present findings suggest that each type of classical cadherin has a distinct CR-organizing activity. These findings provide a new perspective on the higher-order structures of AJs. Because the AJ-based CR was first observed in various types of epithelia in vivo, CRs of epithelial cell sheets have been thought to contain E-cadherin and/or classical cadherins in a ring-like arrangement (Mooseker, 1976; Owaribe et al., 1981). The density of the actin belt in CRs varies with the cell/tissue type, but the mechanism for regulating actin packing in CRs is not well understood. We propose here that the density of the actin belt in CRs might be determined by the balance between the classical cadherins expressed in the AJs of a given cell type. If this is the case, Tara might contribute to the morphogenesis of various parts of the body by spatiotemporally modulating the balance of the classical cadherins.

In conclusion, we found that Tara/Trio RhoGEF/Rac1/p38/Tbx3 is a novel signaling cascade involved in the remodeling of epithelial cell sheets by regulating the transcription of *E-cadherin*. These findings reveal for the first time that the AJ-associated E-cadherin complex regulates the transcription of *E-cadherin*. These discoveries will be critical to fully understand E-cadherin's diverse and specific functions, and to suggest new research directions on the roles of E-cadherin–related signaling cascades. Further analyses of this cascade in vivo and of other signals that regulate *E-cadherin* transcription should elucidate ways to manipulate development-, regeneration-, and/or tumor-related processes for novel strategies in medical therapies. Studies along these lines are being conducted in our laboratory.

## Materials and methods

### Antibodies and reagents

To generate an anti-Tara pAb, rabbits were immunized with a GST-Tara (111–190 aa) fusion protein. Mouse anti–cadherin-6 pAb was a special gift from Dr. M. Takeichi (Center for Developmental Biology, Kobe, Japan) and was generated using cadherin-6 knockout mice. Rat anti-occludin (MOC37) and anti-ZO1 mAbs were generated and characterized in our laboratory (Saitou et al., 1998; Kitajiri et al., 2004). Rat anti–E-cadherin mAb was kindly provided by Dr. M. Takeichi. Mouse anti-HA mAb (Covance), goat anti–ZO-2 pAb, rabbit anti-Trio pAb, rabbit anti-Tbx3 pAb, anti–lamin B pAb (Santa Cruz Biotechnology, Inc.), anti-p38, anti–phospho p38 (Cell Signaling Technology), rabbit anti–claudin-3 pAb (Invitrogen), mouse anti-Rac1 mAb (Millipore), mouse anti-desmoplakin mAb (Progen), mouse anti-Trio pAb (Abnova), and mouse and rabbit anti-Tbx3 pAbs (Abcam) were purchased. Rabbit anti–α-catenin pAb, rabbit anti–β-catenin pAb, mouse anti-vinculin mAb, mouse anti-Flag mAb, and mouse anti–α-tubulin mAb were from Sigma-Aldrich. SB203580 was from EMD. ITX3 was described previously (Bouquier et al., 2009). The Phosphoprotein Colorimetric Assay kit, Pro-Q, was from Invitrogen.

### Plasmids and primers

The cDNA clones encoding Tara and Tbx3 were isolated from a mouse liver and kidney cDNA library. The Tara cDNA was cloned into the pCAGGS-NHA vector, and Tbx3 and its mutant were cloned into the pAcGFP-C1 vector (Takara Bio Inc.). The pGEX4T1-CRIB-Pak used for the pull-down assays of Rac1 was described previously (Matsuo et al., 2002; Ikenouchi et al., 2007). The primers for *E-cadherin* and *GAPDH* used for quantitative RT-PCR and the *E-cadherin* promoter used for luciferase assays were described previously (Behrens et al., 1991; Youn et al., 2005).

### Knockdown constructs

To suppress the expression of Tara in MDCK cells, DNA oligonucleotides of target sequences encoding two distinct portions of the respective ORFs were cloned into an H1 promoter-driven RNAi vector (Brummelkamp et al., 2002). The vectors were transfected into MDCK cells, and suppressed the expression of Tara. Four clones obtained from the two constructs were selected. The probe sequences were: *Tara* (112–130), 5′-GGAGAGTGGAAGAAGCATT-3′; *Tara* (117–135), 5′-GTGGAAAGAAGCATTGGTTT-3′; *Tara* Scramble, 5′-TTACGAAGAAGGTGAGAGG-3′; *Trio* (305–323), 5′-GCATTCATGTTGCACTGAT-3′; *Rac1* (552–570), 5′-GAGGAAGAGAAAATGCCTG-3′. The probe sequences for *E-cadherin* and *cadherin-6* were reported previously (Capaldo and Macara, 2007).

### Cell culture and transfections

MDCK-II and HEK293 cells were grown in DME supplemented with 10% fetal calf serum. Transfection was performed using the Lipofectamine Plus Reagent (Invitrogen), according to the manufacturer's instructions. Most results shown were from transfected MDCK-II cells.

### Immunofluorescence microscopy

MDCK cells were fixed in 1% formalin for 5 min at room temperature. The cells were then treated with 0.2% Triton X-100 in PBS for 5 min and processed for immunofluorescence microscopy as described previously (Yamazaki et al., 2008b). Alexa Fluor 488– or 568–conjugated secondary antibodies were used. For actin staining, Alexa Fluor 568 phalloidin (Invitrogen) was added to the secondary antibody. Specimens were observed at RT with a photomicroscope (BX51 and BX70; Olympus) equipped with a 100x, 1.4 NA oil immersion lens; 60x, 1.42 NA oil immersion lens; and 20x, 0.5 NA lens, and with a confocal microscope (Axiovert 200M; Carl Zeiss, Inc.) equipped with a Plan-Apochromat (63x/1.40 NA oil immersion objective) with appropriate binning of pixels and exposure time. Photographs were recorded with a cooled CCD camera (ORCA-ER, Hamamatsu Photonics; or CoolSnap HQ, Photometrics). The images were analyzed with IPLab version 3.9.5 (BD), MetaMorph (Molecular Devices), LSM510 Meta version 3.0 (Carl Zeiss, Inc.), and Deltavision software

(DeltaVision Core; Applied Precision). Images shown represent maximal intensity projections. Equivalent exposure conditions and scaling was used between controls and Tara-KD cells, and adjusted with only contrast and brightness adjustment.

**GST pull-down and immunoprecipitation**

HEK293 cells were transfected with expression vectors. The lysates from these cells were mixed with GST 4b beads (GE Healthcare) preabsorbed with GST fusion proteins. The nuclei were isolated from MDCK cells as reported previously (Sadowski and Gilman, 1993). In brief, cells were rinsed with ice-cold PBS contaning 1 mM $Na_3VO_4$ and 5 mM sodium fluoride. Ice-cold hypotonic buffer with 0.2% Nonidet P-40 was used as cell lysis buffer. After centrifugation, the nuclei pellets were treated with high salt buffer to remove DNA. The nuclear extracts were prepared and incubated with antibody-conjugated beads for 5 h. Each sample was analyzed by immunoblotting or with a phosphoprotein detection kit.

**Rac1 activity assay**

GTP-loaded Rac1 was measured using a commercially available kit (Thermo Fisher Scientific), as described previously (Nojima et al., 2008).

**Immunoblotting**

To prepare total cell lysates for immunoblotting, MDCK or HEK293 cells were lysed with SDS-PAGE sample buffer, sonicated, and boiled. The protein samples were separated by one-dimensional SDS-PAGE, transferred onto a nitrocellulose or PVDF membrane, and blotted with the appropriate antibodies. For quantification of signals in immunoblotting, the densitometric quantification of immunoblot bands with loading control in the same immunoblotting membranes was performed using Photoshop 7.0 software (Adobe). The immunoblot signals were normalized to the corresponding α-tubulin signal from the same filter, basically by being immunoblotted on the different portions of the same membranes or by being reprobed one by one. In some cases, they were normalized by being immunoblotted at the same time by mixure of antibodies, as specially mentioned in the legends.

**FRET analyses**

Raichu FRET probes for Rac1 were generous gifts from M. Matsuda (Kyoto University, Kyoto, Japan). Raichu probes were transiently transfected into MDCK cells, or Tara-KD cells by using Lipofectamine (Invitrogen) following the manufacturer's recommended procedure. 24 h later, the cells were replated on the glass-bottom dishes. 12, 24, and 48 hours after replating, cells were imaged every 5 min for 2 h with a microscope (IX-81; Olympus) equipped with a 75-W xenon arc lamp, two filter changers, a temperature-controlled chamber, and a cooled charge-coupled device camera (CoolSNAP HQ; Photometrics), controlled by MetaMorph software (Invitrogen). The ratio image of YFP/CFP was created with MetaMorph software and used to represent FRET efficiency.

In the IMD mode images (Ratio), eight colors from red to blue are used to represent the YFP/CFP ratio, with the intensity of each color indicating the mean intensity of YFP and CFP. The upper and lower limits of the ratio range are shown on the right.

**3D culture in collagen gel**

3D cultures were performed in collagen gels (Nitta Gelatin) according to the manufacturer's instructions. In brief, cells were added to a collagen I mixture, gently mixed, and plated onto 12-well transwell insert plates at $5 \times 10^3$ cells/well. 10-d-old cysts were examined for the general cyst architecture as described previously (Pollack et al., 1998).

**Scanning and transmission electron microscopy**

Cells were cultured in Transwell inserts or collagen gels. For scanning electron microscopy, the cells were permeabilized with RIPA buffer after 1% formalin treatment. The images were obtained with a microscope (S-800; Hitachi). The transmission electron microscopy was performed as described previously (Umeda et al., 2006).

**Statistical analysis**

Data are presented as mean ± SD. Whenever necessary, statistical significance of the data was analyzed by performing one-sample *t* tests. The specific types of tests and the P values, when applicable, are indicated in the figure legends.

**Online supplemental material**

Fig. S1 shows additional data on the AJ localization of Tara and additional characterization of Tara-KD cells. Fig. S2 shows additional characterization of Tara-KD cells and of Trio as a binding partner of Tara. Fig. S3 shows additional characterization of the mechanism of Tara-KD–induced down-regulation of E-cadherin. Fig. S4 shows additional analysis of Tara-KD–mediated signals. Fig. S5 shows characterization of cyst formation of Tara-KD cells. Video 1 shows FRET analysis for Raichu-Rac1 in the mock control cells between 11 and 13 h after being seeded. Video 2 shows FRET analysis for Raichu-Rac1 in the mock control cells between 23 and 25 h after being seeded. Video 3 shows FRET analysis for Raichu-Rac1 in the mock control cells between 47 and 49 h after being seeded. Video 4 shows FRET analysis for Raichu-Rac1 in the Tara-KD cells between 11 and 13 h after being seeded. Video 5 shows FRET analysis for Raichu-Rac1 in the mock control cells between 23 and 25 h after being seeded. Video 6 shows FRET analysis for Raichu-Rac1 in the mock control cells between 47 and 49 h after being seeded. Online supplemental material is available at http://www.jcb.org/cgi/content/full/jcb.201009100/DC1.

We are grateful to Dr. Masatoshi Takeichi for the generous gift of the mouse anti–cadherin-6 pAb and for valuable discussions during this study; Drs. Kohei Miyazono and Akira Nagafuchi for helpful discussions; and Dr. Hisashi Nojima for providing the Trio expression plasmids. We also thank Chiyomi Inoue and Orie Koga for their technical assistance and Drs. Grace Gray and Leslie Miglietta for proofreading the manuscript. We further thank all the members of our laboratory for helpful discussions.

This study was supported in part by a Grant-in-Aid for Creative Scientific Research and a Grant-in-Aid for Cancer Research from the Ministry of Education, Science and Culture of Japan to Sachiko Tsukita.

Submitted: 20 September 2010
Accepted: 22 March 2011

## References

Abe, K., and M. Takeichi. 2008. EPLIN mediates linkage of the cadherin catenin complex to F-actin and stabilizes the circumferential actin belt. *Proc. Natl. Acad. Sci. USA*. 105:13–19. doi:10.1073/pnas.0710504105

Abrahams, A., S. Mowla, M.I. Parker, C.R. Goding, and S. Prince. 2008. UV-mediated regulation of the anti-senescence factor Tbx2. *J. Biol. Chem.* 283:2223–2230. doi:10.1074/jbc.M705651200

Backer, S., M. Hidalgo-Sánchez, N. Offner, E. Portales-Casamar, A. Debant, P. Fort, C. Gauthier-Rouvière, and E. Bloch-Gallego. 2007. Trio controls the mature organization of neuronal clusters in the hindbrain. *J. Neurosci.* 27:10323–10332. doi:10.1523/JNEUROSCI.1102-07.2007

Behrens, J., O. Löwrick, L. Klein-Hitpass, and W. Birchmeier. 1991. The E-cadherin promoter: functional analysis of a G.C-rich region and an epithelial cell-specific palindromic regulatory element. *Proc. Natl. Acad. Sci. USA*. 88: 11495–11499. doi:10.1073/pnas.88.24.11495

Bouquier, N., E. Vignal, S. Charrasse, M. Weill, S. Schmidt, J.P. Léonetti, A. Blangy, and P. Fort. 2009. A cell active chemical GEF inhibitor selectively targets the Trio/RhoG/Rac1 signaling pathway. *Chem. Biol.* 16:657–666. doi:10.1016/j.chembiol.2009.04.012

Braga, V.M. 2002. Cell-cell adhesion and signalling. *Curr. Opin. Cell Biol.* 14:546–556. doi:10.1016/S0955-0674(02)00373-3

Brembeck, F.H., M. Rosário, and W. Birchmeier. 2006. Balancing cell adhesion and Wnt signaling, the key role of beta-catenin. *Curr. Opin. Genet. Dev.* 16:51–59. doi:10.1016/j.gde.2005.12.007

Brummelkamp, T.R., R. Bernards, and R. Agami. 2002. A system for stable expression of short interfering RNAs in mammalian cells. *Science*. 296:550–553. doi:10.1126/science.1068999

Capaldo, C.T., and I.G. Macara. 2007. Depletion of E-cadherin disrupts establishment but not maintenance of cell junctions in Madin-Darby canine kidney epithelial cells. *Mol. Biol. Cell*. 18:189–200. doi:10.1091/mbc.E06-05-0471

Charrasse, S., F. Comunale, M. Fortier, E. Portales-Casamar, A. Debant, and C. Gauthier-Rouvière. 2007. M-cadherin activates Rac1 GTPase through the Rho-GEF trio during myoblast fusion. *Mol. Biol. Cell*. 18:1734–1743. doi:10.1091/mbc.E06-08-0766

Chen, Y.T., D.B. Stewart, and W.J. Nelson. 1999. Coupling assembly of the E-cadherin/β-catenin complex to efficient endoplasmic reticulum exit and basal-lateral membrane targeting of E-cadherin in polarized MDCK cells. *J. Cell Biol.* 144:687–699. doi:10.1083/jcb.144.4.687

Debant, A., C. Serra-Pagès, K. Seipel, S. O'Brien, M. Tang, S.H. Park, and M. Streuli. 1996. The multidomain protein Trio binds the LAR transmembrane tyrosine phosphatase, contains a protein kinase domain, and has separate rac-specific and rho-specific guanine nucleotide exchange factor domains. *Proc. Natl. Acad. Sci. USA*. 93:5466–5471. doi:10.1073/pnas.93.11.5466

Etienne-Manneville, S., and A. Hall. 2002. Rho GTPases in cell biology. *Nature*. 420:629–635. doi:10.1038/nature01148

Gumbiner, B.M. 2005. Regulation of cadherin-mediated adhesion in morphogenesis. *Nat. Rev. Mol. Cell Biol.* 6:622–634. doi:10.1038/nrm1699

Hage, B., K. Meinel, I. Baum, K. Giehl, and A. Menke. 2009. Rac1 activation inhibits E-cadherin-mediated adherens junctions via binding to IQGAP1 in pancreatic carcinoma cells. *Cell Commun. Signal.* 7:23. doi:10.1186/1478-811X-7-23

Halbleib, J.M., and W.J. Nelson. 2006. Cadherins in development: cell adhesion, sorting, and tissue morphogenesis. *Genes Dev.* 20:3199–3214. doi:10.1101/gad.1486806

Heasman, S.J., and A.J. Ridley. 2008. Mammalian Rho GTPases: new insights into their functions from in vivo studies. *Nat. Rev. Mol. Cell Biol.* 9:690–701. doi:10.1038/nrm2476

Ikenouchi, J., M. Matsuda, M. Furuse, and S. Tsukita. 2003. Regulation of tight junctions during the epithelium-mesenchyme transition: direct repression of the gene expression of claudins/occludin by Snail. *J. Cell Sci.* 116:1959–1967. doi:10.1242/jcs.00389

Ikenouchi, J., K. Umeda, S. Tsukita, M. Furuse, and S. Tsukita. 2007. Requirement of ZO-1 for the formation of belt-like adherens junctions during epithelial cell polarization. *J. Cell Biol.* 176:779–786. doi:10.1083/jcb.200612080

Ireton, R.C., M.A. Davis, J. van Hengel, D.J. Mariner, K. Barnes, M.A. Thoreson, P.Z. Anastasiadis, L. Matrisian, L.M. Bundy, L. Sealy, et al. 2002. A novel role for p120 catenin in E-cadherin function. *J. Cell Biol.* 159:465–476. doi:10.1083/jcb.200205115

Itoh, M., S. Nagafuchi, S. Moroi, and S. Tsukita. 1997. Involvement of ZO-1 in cadherin-based cell adhesion through its direct binding to alpha catenin and actin filaments. *J. Cell. Biol.* 138:181–192.

Jeanes, A., C.J. Gottardi, and A.S. Yap. 2008. Cadherins and cancer: how does cadherin dysfunction promote tumor progression? *Oncogene*. 27:6920–6929. doi:10.1038/onc.2008.343

Kashef, J., A. Köhler, S. Kuriyama, D. Alfandari, R. Mayor, and D. Wedlich. 2009. Cadherin-11 regulates protrusive activity in Xenopus cranial neural crest cells upstream of Trio and the small GTPases. *Genes Dev.* 23:1393–1398. doi:10.1101/gad.519409

Khanna, P., T. Yunkunis, H.S. Muddana, H.H. Peng, A. August, and C. Dong. 2010. p38 MAP kinase is necessary for melanoma-mediated regulation of VE-cadherin disassembly. *Am. J. Physiol. Cell Physiol.* 298:C1140–C1150. doi:10.1152/ajpcell.00242.2009

Kitajiri, S., T. Miyamoto, A. Mineharu, N. Sonoda, K. Furuse, M. Hata, H. Sasaki, Y. Mori, T. Kubota, J. Ito, et al. 2004. Compartmentalization established by claudin-11-based tight junctions in stria vascularis is required for hearing through generation of endocochlear potential. *J. Cell Sci.* 117:5087–5096. doi:10.1242/jcs.01393

Lecuit, T. 2005. Adhesion remodeling underlying tissue morphogenesis. *Trends Cell Biol.* 15:34–42. doi:10.1016/j.tcb.2004.11.007

Lozano, E., M.A. Frasa, K. Smolarczyk, U.G. Knaus, and V.M. Braga. 2008. PAK is required for the disruption of E-cadherin adhesion by the small GTPase Rac. *J. Cell Sci.* 121:933–938. doi:10.1242/jcs.016121

Matsuo, N., M. Hoshino, M. Yoshizawa, and Y. Nabeshima. 2002. Characterization of STEF, a guanine nucleotide exchange factor for Rac1, required for neurite growth. *J. Biol. Chem.* 277:2860–2868. doi:10.1074/jbc.M106186200

Mège, R.M., J. Gavard, and M. Lambert. 2006. Regulation of cell-cell junctions by the cytoskeleton. *Curr. Opin. Cell Biol.* 18:541–548. doi:10.1016/j.ceb.2006.08.004

Nishimura, T., and M. Takeichi. 2009. Remodeling of the adherens junctions during morphogenesis. *Curr. Top. Dev. Biol.* 89:33–54. doi:10.1016/S0070-2153(09)89002-9

Mooseker, M.S. 1976. Brush border motility. Microvillar contraction in triton-treated brush borders isolated from intestinal epithelium. *J. Cell Biol.* 71:417–433. doi:10.1083/jcb.71.2.417

Nojima, H., M. Adachi, T. Matsui, K. Okawa, S. Tsukita, and S. Tsukita. 2008. IQGAP3 regulates cell proliferation through the Ras/ERK signalling cascade. *Nat. Cell Biol.* 10:971–978. doi:10.1038/ncb1757

Otani, T., T. Ichii, S. Aono, and M. Takeichi. 2006. Cdc42 GEF Tuba regulates the junctional configuration of simple epithelial cells. *J. Cell Biol.* 175:135–146. doi:10.1083/jcb.200605012

Owaribe, K., R. Kodama, and G. Eguchi. 1981. Demonstration of contractility of circumferential actin bundles and its morphogenetic significance in pigmented epithelium in vitro and in vivo. *J. Cell Biol.* 90:507–514. doi:10.1083/jcb.90.2.507

Papaioannou, V.E., and L.M. Silver. 1998. The T-box gene family. *Bioessays*. 20:9–19. doi:10.1002/(SICI)1521-1878(199801)20:1<9::AID-BIES4>3.0.CO;2-Q

Pokutta, S., and W.I. Weis. 2007. Structure and mechanism of cadherins and catenins in cell-cell contacts. *Annu. Rev. Cell. Dev. Biol.* 23:237–261. doi:10.1146/annurev.cellbio.22.010305.104241

Perez-Moreno, M., C. Jamora, and E. Fuchs. 2003. Sticky business: orchestrating cellular signals at adherens junctions. *Cell*. 112:535–548. doi:10.1016/S0092-8674(03)00108-9

Pollack, A.L., R.B. Runyan, and K.E. Mostov. 1998. Morphogenetic mechanisms of epithelial tubulogenesis: MDCK cell polarity is transiently rearranged without loss of cell-cell contact during scatter factor/hepatocyte growth factor-induced tubulogenesis. *Dev. Biol.* 204:64–79. doi:10.1006/dbio.1998.9091

Renard, C.A., C. Labalette, C. Armengol, D. Cougot, Y. Wei, S. Cairo, P. Pineau, C. Neuveut, A. de Reyniès, A. Dejean, et al. 2007. Tbx3 is a downstream target of the Wnt/β-catenin pathway and a critical mediator of β-catenin survival functions in liver cancer. *Cancer Res.* 67:901–910. doi:10.1158/0008-5472.CAN-06-2344

Rodriguez, M., E. Aladowicz, L. Lanfrancone, and C.R. Goding. 2008. Tbx3 represses E-cadherin expression and enhances melanoma invasiveness. *Cancer Res.* 68:7872–7881. doi:10.1158/0008-5472.CAN-08-0301

Rygiel, T.P., A.E. Mertens, K. Strumane, R. van der Kammen, and J.G. Collard. 2008. The Rac activator Tiam1 prevents keratinocyte apoptosis by controlling ROS-mediated ERK phosphorylation. *J. Cell Sci.* 121:1183–1192. doi:10.1242/jcs.017194

Sadowski, H.B., and M.Z. Gilman. 1993. Cell-free activation of a DNA-binding protein by epidermal growth factor. *Nature*. 362:79–83. doi:10.1038/362079a0

Saitou, M., K. Fujimoto, Y. Doi, M. Itoh, T. Fujimoto, M. Furuse, H. Takano, T. Noda, and S. Tsukita. 1998. Occludin-deficient embryonic stem cells can differentiate into polarized epithelial cells bearing tight junctions. *J. Cell Biol.* 141:397–408. doi:10.1083/jcb.141.2.397

Schmidt, A., and A. Hall. 2002. Guanine nucleotide exchange factors for Rho GTPases: turning on the switch. *Genes Dev.* 16:1587–1609. doi:10.1101/gad.1003302

Seipel, K., S.P. O'Brien, E. Iannotti, Q.G. Medley, and M. Streuli. 2001. Tara, a novel F-actin binding protein, associates with the Trio guanine nucleotide exchange factor and regulates actin cytoskeletal organization. *J. Cell Sci.* 114:389–399.

Stewart, D.B., A.I. Barth, and W.J. Nelson. 2000. Differential regulation of endogenous cadherin expression in Madin-Darby canine kidney cells by cell-cell adhesion and activation of β -catenin signaling. *J. Biol. Chem.* 275:20707–20716. doi:10.1074/jbc.M000467200

Takeichi, M. 1995. Morphogenetic roles of classic cadherins. *Curr. Opin. Cell Biol.* 7:619–627. doi:10.1016/0955-0674(95)80102-2

Tsukita, S., and S. Tsukita. 1989. Isolation of cell-to-cell adherens junctions from rat liver. *J. Cell Biol.* 108:31–41. doi:10.1083/jcb.108.1.31

Umeda, K., J. Ikenouchi, S. Katahira-Tayama, K. Furuse, H. Sasaki, M. Nakayama, T. Matsui, S. Tsukita, M. Furuse, and S. Tsukita. 2006. ZO-1 and ZO-2 independently determine where claudins are polymerized in tight-junction strand formation. *Cell*. 126:741–754. doi:10.1016/j.cell.2006.06.043

Wheelock, M.J., Y. Shintani, M. Maeda, Y. Fukumoto, and K.R. Johnson. 2008. Cadherin switching. *J. Cell Sci.* 121:727–735. doi:10.1242/jcs.000455

Yamazaki, Y., K. Okawa, T. Yano, S. Tsukita, and S. Tsukita. 2008a. Optimized proteomic analysis on gels of cell-cell adhering junctional membrane proteins. *Biochemistry*. 47:5378–5386. doi:10.1021/bi8002567

Yamazaki, Y., K. Umeda, M. Wada, S. Nada, M. Okada, S. Tsukita, and S. Tsukita. 2008b. ZO-1- and ZO-2-dependent integration of myosin-2 to epithelial zonula adherens. *Mol. Biol. Cell*. 19:3801–3811. doi:10.1091/mbc.E08-04-0352

Yonemura, S., M. Itoh, A. Nagafuchi, and S. Tsukita. 1995. Cell-to-cell adherens junction formation and actin filament organization: similarities and differences between non-polarized fibroblasts and polarized epithelial cells. *J. Cell. Sci.* 108:127–142.

Youn, Y.H., J. Hong, and J.M. Burke. 2005. Endogenous N-cadherin in a subpopulation of MDCK cells: distribution and catenin complex composition. *Exp. Cell Res.* 303:275–286. doi:10.1016/j.yexcr.2004.09.023

Zhang, Y., L.A. Rivera Rosado, S.Y. Moon, and B. Zhang. 2009. Silencing of D4-GDI inhibits growth and invasive behavior in MDA-MB-231 cells by activation of Rac-dependent p38 and JNK signaling. *J. Biol. Chem.* 284:12956–12965. doi:10.1074/jbc.M807845200

Zohn, I.E., Y. Li, E.Y. Skolnik, K.V. Anderson, J. Han, and L. Niswander. 2006. p38 and a p38-interacting protein are critical for downregulation of E-cadherin during mouse gastrulation. *Cell*. 125:957–969. doi:10.1016/j.cell.2006.03.048